

Molecule-Based Magnets: Ferro- and Antiferromagnetic Interactions in Copper(II)–Polyorganosiloxanolate Clusters

Eva Rentschler,^{1a} Dante Gatteschi,^{*,1a} Andrea Cornia,^{1b} Antonio C. Fabretti,^{1b} Anne-Laure Barra,^{1c} Olga I. Shchegolikhina,^{1d} and Alexandr A. Zhdanov^{1d}

Department of Chemistry, University of Florence, via Maragliano 75, 50144 Firenze, Italy, Department of Chemistry, University of Modena, via G. Campi 183, 41100 Modena, Italy, Laboratoire des Champs Magnetiques Intenses, CNRS, Grenoble, France, and A. N. Nesmeyanov Institute of Organoelement Compounds (INEOS), 28 Vavilov St., Moscow 117813, Russia

Received October 16, 1995[⊗]

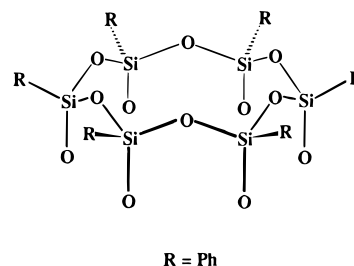
The magnetic behavior of the clusters $[(\text{PhSiO}_2)_6\text{Cu}_6(\text{O}_2\text{SiPh})_6] \cdot 6\text{EtOH}$ (**1**), $\text{Na}_4[(\text{PhSiO}_2)_{12}\text{Cu}_4] \cdot 8^o\text{BuOH}$ (**2**), and $\text{K}_4[(\text{C}_2\text{H}_3\text{SiO}_2)_{12}\text{Cu}_4] \cdot 6^o\text{BuOH}$ (**3**) has been investigated by combined magnetic susceptibility measurements and variable-temperature EPR techniques (9.25 and 245 GHz). The six copper(II) ions in the core of **1**, which approaches $6/mmm$ symmetry, are ferromagnetically coupled as a result of the geometry at the bridging siloxanolate oxygen atoms ($\text{Cu}-\text{O}-\text{Cu} = 91.5-94.6^\circ$; $J = -42 \text{ cm}^{-1}$ with $\mathbf{H} = J \sum_{i=1}^6 \mathbf{S}_i \cdot \mathbf{S}_{i+1}$, $\mathbf{S}_7 = \mathbf{S}_1$). The ground $S = 3$ spin state is split in zero field mainly due to anisotropic exchange contributions ($D = 0.30 \text{ cm}^{-1}$). Notably, both the magnitude and the sign of the zero-field splitting parameter have been determined from HF-EPR spectra. Large antiferromagnetic Cu-Cu interactions ($J \sim 200 \text{ cm}^{-1}$) and an $S = 0$ ground state have been detected in the tetranuclear clusters **2** and **3** as a consequence of the larger Cu-O-Cu angles. The results presented in the paper are relevant to the search for new molecule-based magnetic materials.

Introduction

Large metal ion clusters are currently intensively investigated, for many different purposes, ranging from the design of new magnetic materials of nanometric size² to the interest for the mechanism of biomineralization.³ One of the challenges to be met in order to grow large clusters is that of finding suitable ligands which can prevent the growth of finite size particles. Up to now many different ligands have been used for this purpose, like carboxylates,⁴ polyketonates,⁵ amines,⁶ etc.

A new class of ligands has been recently produced using polysiloxanates,⁷ which have been found to be particularly attractive for their ability of combining the properties of the inorganic and organic moieties which constitute them. In fact they are polymeric, due to the formation of O-Si-O networks, and their properties can in principle be fine tuned by substitutions on the aromatic moieties.

A particularly suitable ligand is the hexaphenylcyclohexasiloxanolate ligand $[(\text{PhSiO}_2^-)_6]$ (structure **I**). Two such ligands



form sandwich-like complexes by coordinating up to eight metal ions. In all the sandwich-like polymetallaorganosiloxanolate (PMOS) complexes described up to now,⁷ additional solvent molecules coordinate the transition metal atoms, expanding the coordination number. In most cases the molecules are additionally stabilized by encapsulating bridging anionic ligands like $\mu_6\text{-Cl}^-$, $\mu_3\text{-OH}^-$, and $\mu_3\text{-O}^{2-}$ in the metal layer.^{7a-d,f} We have previously shown that the encapsulated group has a relevant role for the mechanism of exchange between metal ions like nickel(II).^{7f} We wish to report here the magnetic properties of a hexanuclear complex $[(\text{PhSiO}_2)_6\text{Cu}_6(\text{O}_2\text{SiPh})_6] \cdot 6\text{EtOH}$ (**1**)^{7c} and two tetranuclear complexes $\text{Na}_4[(\text{PhSiO}_2)_{12}\text{Cu}_4] \cdot 8^o\text{BuOH}$ (**2**) and $\text{K}_4[(\text{C}_2\text{H}_3\text{SiO}_2)_{12}\text{Cu}_4] \cdot 6^o\text{BuOH}$ (**3**),^{7e} which do not contain encapsulated ions due to the low tendency of copper(II) to form octahedral complexes.

* To whom correspondence should be addressed.

⊗ Abstract published in *Advance ACS Abstracts*, June 15, 1996.

- (1) (a) University of France. (b) University of Modena. (c) CNRS, Grenoble. (d) INEOS.
- (2) (a) Gatteschi, D. *Adv. Mater.* **1994**, *6*, 635. (b) Gatteschi, D.; Caneschi, A.; Pardi, L.; Sessoli, R. *Science* **1994**, *265*, 1054. (c) Awschalom, D. D.; Di Vincenzo, D. P.; Smyth, J. F. *Science* **1992**, *258*, 414.
- (3) (a) *Biomineralization: Chemical and Biochemical Perspectives*; Mann, S., Webb, J., Williams, R. J. P., Eds., VCH: New York, 1988. (b) Meldrun, F. C.; Heywood, B. R.; Mann, S. *Science* **1992**, *257*, 522.
- (4) (a) Wieghardt, K. *Angew. Chem., Int. Ed. Engl.* **1989**, *28*, 1153. (b) Lippard, S. J. *Angew. Chem., Int. Ed. Engl.* **1988**, *27*, 344.
- (5) (a) Taft, K. L.; Caneschi, A.; Pence, L. E.; Papaefthymiou, G.; Delfs, C. D.; Lippard, S. J. *J. Am. Chem. Soc.* **1993**, *115*, 11753. (b) Caneschi, A.; Cornia, A.; Lippard, S. J. *Angew. Chem., Int. Ed. Engl.* **1995**, *34*, 467. (c) Caneschi, A.; Cornia, A.; Fabretti, A. C.; Gatteschi, D. *Angew. Chem., Int. Ed. Engl.* **1995**, *34*, 2862.
- (6) (a) Powell, A. K.; Heath, S. L.; Gatteschi, D.; Pardi, L.; Sessoli, R.; Spina, G.; Del Giallo, F.; Pieralli, F. *J. Am. Chem. Soc.* **1995**, *117*, 2491. (b) Hagen, K. S.; Armstrong, W. H.; Olmstead, M. M. *J. Am. Chem. Soc.* **1989**, *111*, 774.

- (7) (a) Shchegolikhina, O. I.; Zhdanov, A. A.; Igonin, V. A.; Ovchinnikov, Yu. E.; Shklover, V. E.; Struchkov, Yu. T. *Organomet. Chem. USSR* **1991**, *4*, 39. (b) Levitsky, M. M.; Shchegolikhina, O. I.; Zhdanov, A. A.; Igonin, V. A.; Ovchinnikov, Yu. E.; Shklover, V. E.; Struchkov, Yu. T. *J. Organomet. Chem.* **1991**, *401*, 199. (c) Igonin, V. A.; Shchegolikhina, O. I.; Lindeman, S. V.; Levitsky, M. M.; Struchkov, Yu. T.; Zhdanov, A. A. *J. Organomet. Chem.* **1992**, *423*, 351. (d) Igonin, V. A.; Lindeman, S. V.; Potekhin, K. A.; Shklover, V. E.; Struchkov, Yu. T.; Shchegolikhina, O. I.; Zhdanov, A. A.; Razumovskaya, I. V. *Organomet. Chem. USSR* **1991**, *4*, 383. (e) Igonin, V. A.; Lindeman, S. V.; Struchkov, Yu. T.; Shchegolikhina, O. I.; Zhdanov, A. A.; Molodtsova, Yu. A.; Razumovskaya, I. V. *Organomet. Chem. USSR* **1991**, *4*, 672. (f) Cornia, A.; Fabretti, A. C.; Gatteschi, D.; Pályi, G.; Rentschler, E.; Shchegolikhina, O. I.; Zhdanov, A. A. *Inorg. Chem.* **1995**, *34*, 5383.

Experimental Section

Synthesis. All three complexes were prepared by following procedures described elsewhere.^{7c,e}

Instrumentation and Physical Measurements. Magnetic susceptibilities of microcrystalline samples were measured using a Métrologique Ingénierie MS03 SQUID magnetometer in the temperature range 50–260 K for compound **1** and 2.6–280 and 2.5–270 K for compounds **2** and **3**, respectively, with an applied field of 1 T. Further measurements were made in the range 2.2–50 K for compound **1** with an applied field of 0.1 T. The contribution of the sample holder was determined separately in the same temperature range and field. Diamagnetic corrections were estimated from Pascal's constants.

EPR spectra of **1** as a powdered sample were obtained with a Varian E9 spectrometer operating at X-band frequency, equipped with an Oxford Instruments ESR9 liquid helium continuous flow cryostat. The high frequency EPR spectra have been recorded on a laboratory-made spectrometer. An optically pumped far-infrared laser is used as the radiation source. The derivative of the absorption of the far-IR radiation is recorded by a In–Sb bolometer.⁸

Calculations. The calculations for the fittings of the magnetic data were performed on RISC computers, using the program Clumag.⁹ $R = \sum_i [\chi_m T_i^{\text{obs}} - \chi_m T_i^{\text{calcd}}]^2 / \sum_i [\chi_m T_i^{\text{obs}}]^2$ was minimized in the least-squares cycles.

Calculation of the spectra at X-band frequency has been carried out by matrix diagonalization of the full Hamiltonian matrix,¹⁰ assuming $g_{\perp} = 2.22$ and $g_{\parallel} = 2.05$. The high frequency spectra (245 GHz) have been simulated by assuming $g_{\perp} = 2.221$ and $g_{\parallel} = 2.055$ with anisotropic line width $\Delta H_{\perp} = 300$ mT and $\Delta H_{\parallel} = 450$ mT, whereas the zfs term of the spin Hamiltonian has been treated as a second order perturbation to the Zeeman term. The thermal population of the different M levels has been taken into account as a function of the applied magnetic field.

Results and Discussion

Structural Properties. In general, the Si–O and Cu–O bond lengths have similar characteristics as in the nickel-containing siloxanolate complexes previously described.^{7f} In the further discussion the oxygen atoms of the siloxanolate ligand bound to the metal atoms will be indicated as O_m , whereas the others belonging to the ligand will be written as O_c .

In the hexanuclear complex **1** the distances^{7c} in the Cu, O skeleton, which approaches $6/mmm$ symmetry, show only minor variations. The Cu atoms are coordinated by four O_m in an approximately square-planar fashion with bond lengths between 1.92(2) and 1.98(2) Å, which nicely compare with the sum of the ionic radii of O^{2-} and square-planar Cu^{2+} (1.93 Å).¹¹ A long bond (2.34, 2.38 Å) to the solvent oxygen atom gives rise to a distorted tetragonal pyramidal coordination of the Cu^{2+} ions. The angles at the bridging oxygen atoms O_m are found in the range 91.5–94.6°. Intermolecular contacts are observed between the carbon atoms of the phenyl rings along the hexagonal crystal axis with distances down to 3.38 Å. Fewer intermolecular contacts are observed between the oxygen atoms of the siloxanolate ligand and phenyl carbon atoms but even they are well below 4 Å. The crystal packing is shown in Figure 2.

In contrast to the complex **1** and the nickel siloxanolate complexes described earlier,^{7f} the two copper complexes $Na_4[(PhSiO_2)_{12}Cu_4] \cdot 8^oBuOH$ (**2**) and $K_4[(C_2H_3SiO_2)_{12}Cu_4] \cdot 6^oBuOH$ (**3**) contain as basic structural units the cyclododecasiloxanolate ligands, $L = -[PhSiO_2]_{12}$ and $-[C_2H_2SiO_2]_{12}$, respectively,^{7c} as shown in Figure 3. In both complexes these 24-membered cyclic ligands coordinate with their exocyclic oxygen atoms, O_m , four Cu atoms which are placed on the

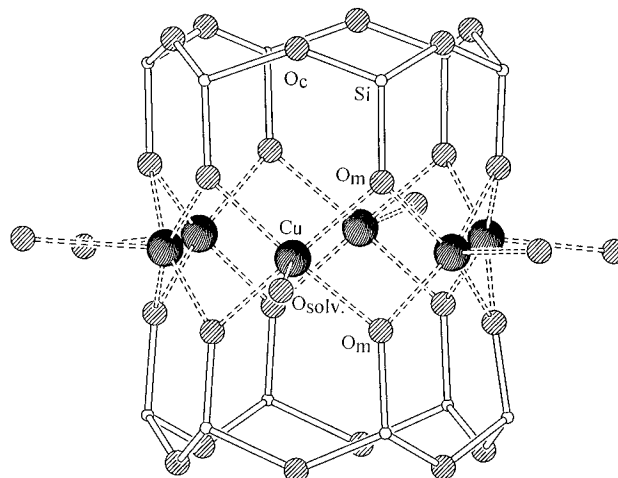


Figure 1. Structure of complex **1**. The phenyl rings of the cyclohexasiloxanolate ligands and the alkyl chains of the ethanol molecules have been omitted for clarity. Average bond lengths and angles are as follows: Cu– O_m 1.94(2) Å, Cu– O_{solv} 2.36(2) Å, Si– O_m 1.64(3) Å, Si– O_c 1.62(2) Å; O_m –Cu– O_m 88.7(9)°, O_m –Cu– O_{solv} 98.3(9)°, Cu– O_m –Cu 92.8(9)°, O_m –Si– O_c 110(1)°, O_c –Si– O_c 110(1)°.

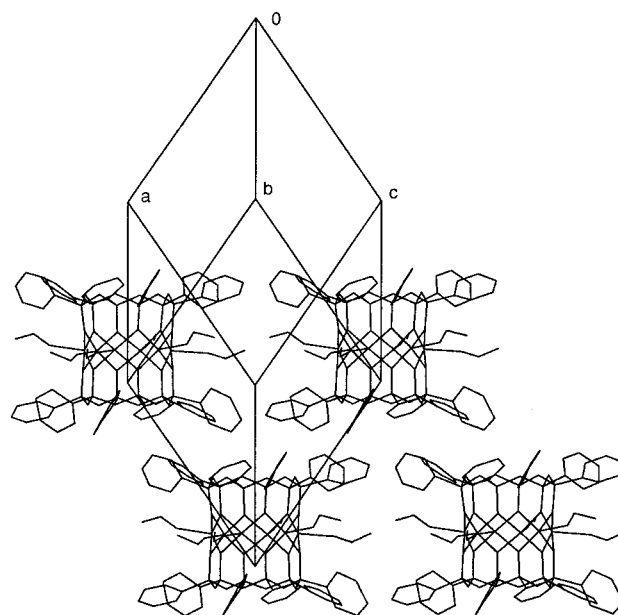


Figure 2. Crystal packing of **1**.

vertices of an elongated tetrahedron. As shown in Figure 3, these tetrahedra are built up by two almost parallel Cu_2O_2 units placed crosswise. In contrast to the tetragonal-pyramidal coordination in **1**, the Cu atoms have here a square planar coordination. The average Cu–O distances (1.92 and 1.94 Å for **2** and **3**, respectively) correspond to the reported sum of the ionic radii, as for **1**.¹¹ The angles at the bridging oxygen atoms, Cu– O_1 –Cu' (**2**) and Cu– O_2 –Cu' (**3**) are widened up to 101.7(3) and 101.2(4)°, respectively. The Cu–Cu distances in the Cu_2O_6 units are found to be 3.02 and 3.06 Å, whereas the distances between these dimeric units are 3.899(3) Å, **2**, and 3.386(3) Å, **3**. In both cases the distances between the dimeric units are such as to exclude apical coordination of a Cu atom by an O atom of the neighboring Cu_2O_2 unit.

Magnetic Properties. The magnetic behavior of **1** is shown in Figure 4 as a χT vs T plot. The value of χT increases upon cooling from 2.8 $emu \cdot K \cdot mol^{-1}$ at 260 K tending to a plateau of 5.80 $emu \cdot K \cdot mol^{-1}$ below 8 K. This description corresponds to a pattern of moderate ferromagnetic coupling in which the highest value of χT is near to that expected for a spin-aligned $S = 3$ ground state (6.0 $emu \cdot K \cdot mol^{-1}$), in which all six spins

(8) Barra, A. L.; Brunel, L. C.; Robert, J. B. *Chem. Phys. Lett.* **1990**, 165, 107.

(9) Gatteschi D.; Pardi L. *Gazz. Chim. Ital.* **1993**, 123, 231.

(10) The program to calculate the intensities of the transitions has been kindly provided by H. Weihe, Inst. f. anorg. u. phys. Chemie, Bern, Switzerland.

(11) Shannon, R. *Acta Crystallogr., Sect. A* **1976**, 32, 75.

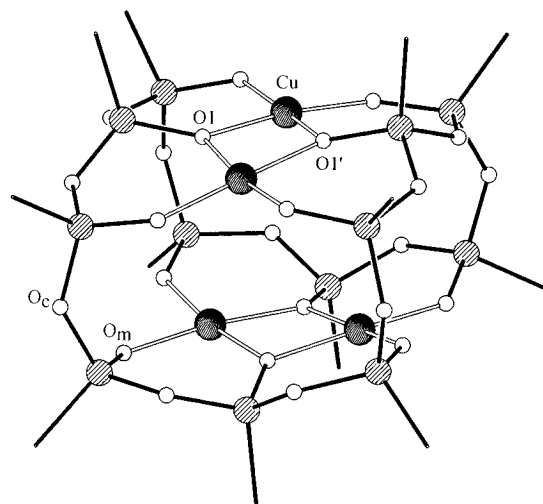


Figure 3. Structure of the core of complexes **2** and **3**. The phenyl rings and vinyl chains of the cyclododecasiloxanolate ligands have been omitted for clarity. Averaged bond length and angles are: Cu–O_m 1.916(7), Si–O_m 1.600(8), Si–O_c 1.642(7), Cu–O_m–Cu 101.7(3)° for **2** and Cu–O_m 1.938(9), Si–O_m 1.60(1), Si–O_c 1.63(1), Cu–O_m–Cu 101.2(4)° for **3**.

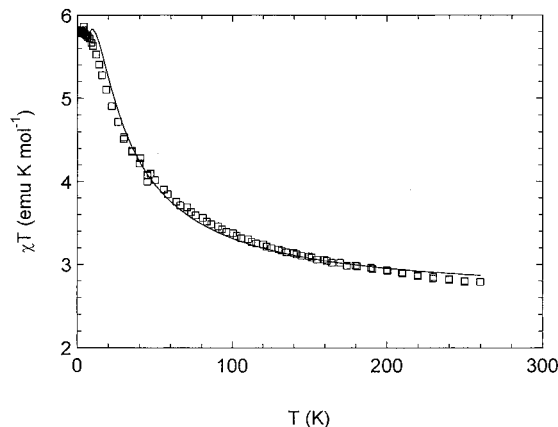


Figure 4. Temperature dependence of χT for compound **1**. The solid line represents the calculated values with the best fit parameters $g = 2.14$, $J = -42.0 \text{ cm}^{-1}$ and $\theta = -0.045 \text{ cm}^{-1}$ (see also text).

are parallel to each other. Taking into consideration only the data above 40 K the χT curve could be well reproduced using the Hamiltonian

$$H = J \sum_{i=1}^6 \mathbf{S}_i \cdot \mathbf{S}_{i+1} \quad (1)$$

where $i + 1 = 7$ is equivalent to $i = 1$.

The data at low temperature are well below the curve resulting from the obtained values of g and J . This effect can in principle be explained through intermolecular contacts, which are remarkable, as outlined above, or by zero field splitting effects of the ground S state. We took them into account by a Weiss correction at low temperature.¹²

$$\chi = \frac{Ng^2\beta^2S(S+1)}{3kT - \theta} \quad (2)$$

where $S = 3$. The best fit values are $g = 2.14$, $J = -42.0 \text{ cm}^{-1}$, and $\theta = -0.045 \text{ cm}^{-1}$ as shown in Figure 4.

The resulting value of J is only in qualitative accordance with the linear correlation

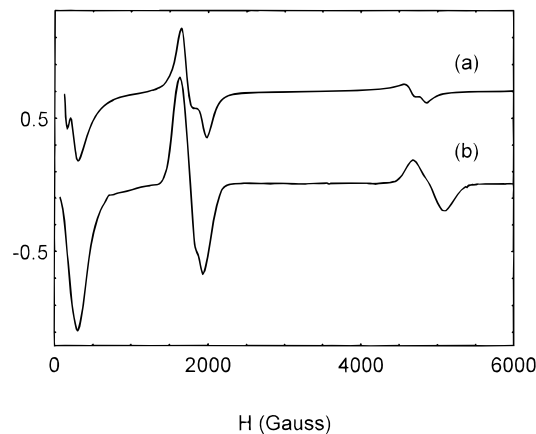


Figure 5. EPR spectra of a polycrystalline powder of **1** at 9.25 GHz: (a) calculated, assuming $S = 3$, $g_{\perp} = 2.221$, $g_{\parallel} = 2.055$, and $D = 0.3 \text{ cm}^{-1}$; (b) recorded at 4 K.

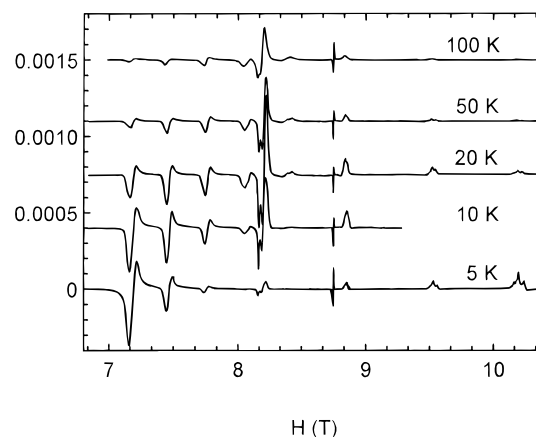


Figure 6. High frequency EPR spectra (245 GHz) of polycrystalline powder of **1** pressed in a pellet at different temperatures.

$$-J (\text{cm}^{-1}) = -74\alpha(^{\circ}) + 7270 \quad (3)$$

reported by Hatfield and Hodgson for bis(μ -hydroxo)-bridged copper(II) complexes, where α represents the Cu–O–Cu bridging angle.¹³ The correlation predicts that for $\alpha < 97.5^{\circ}$ the ground state is a triplet. The here observed deviation of the absolute value of J from the expected one (200–250 cm^{-1}) can be explained due to the nonplanarity of the CuO₂Cu group, which includes angles of 153° and 149° between the planes O₁–Cu₁–O₈, O₁–Cu₂–O₈ and O₂–Cu₁–O₇, O₂–Cu₂–O₇, respectively.

In order to obtain first hand information on the splitting of the ground $S = 3$ state, we recorded EPR spectra at liquid helium temperature. At X-band frequency (9.25 GHz) a strong absorption near zero field is observed (Figure 5) suggesting that two levels are separated by ca. 0.3 cm^{-1} . Assuming axial symmetry the involved zero field split levels can be $M = \pm 3$ and ± 2 , or ± 2 and ± 1 , or ± 1 and 0. Therefore the zero field splitting parameter may correspond to $D \approx M \times 0.3 \text{ cm}^{-1}$, where $M = 5, 3, 1$. The last option seems the most probable.

In order to obtain an unambiguous assignment we recorded also high frequency EPR, HF-EPR, spectra with an exciting frequency of 245 GHz. In Figure 6 are shown the HF-EPR spectra for several temperatures ranging from 5 to 100 K. The spectra at high temperature clearly show the advantage of HF-EPR on conventional EPR. In fact at least four equally spaced transitions are observed at low field, a clear indication of a fine structure for a spin multiplet with $S \geq 2$. The relative intensities

(12) O'Connor, C. J. *Prog. Inorg. Chem.* **1982**, 29, 203.

(13) Crawford, W. H.; Richardson, H. W.; Wasson, J. R.; Hodgson, D. J.; Hatfield, W. E. *Inorg. Chem.* **1976**, 15, 2107.

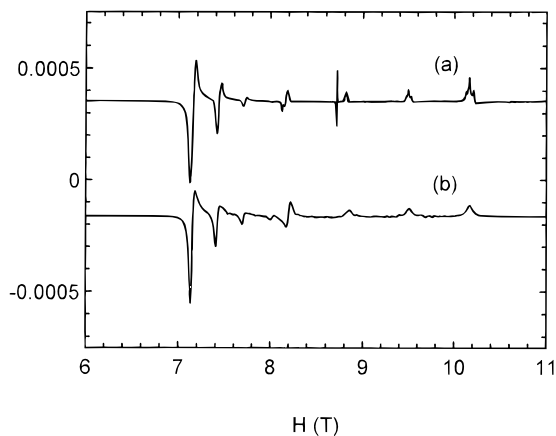


Figure 7. High frequency EPR spectra (245 GHz) of polycrystalline powder of **1** at 5 K: (a) recorded; (b) calculated, assuming $S = 3$, $g_{\perp} = 2.221$, $g_{\parallel} = 2.055$, $D = 0.3 \text{ cm}^{-1}$, $D/E = 0$, and line widths = 300 mT for the transitions perpendicular to the field and 450 mT parallel to the field.

of the lines change dramatically on decreasing temperature, with a marked increase in the relative intensity of the features at the extreme of the spectrum, at 7.2 and 10.2 T respectively.

At 245 GHz the Zeeman energy, $g\mu_B B_0$, is 12 K, therefore depopulation effects of the M levels must be observed at low temperature. Indeed, at 4 K only transitions from the lowest lying states are observed and the pattern of the transition provides the sign of the zero field splitting.¹⁴

In the strong field approximation the resonance fields at low temperature are given by

$$\begin{aligned} H_{\parallel} &= (g_{\parallel}/g_{\parallel})[H_0 + (2S - 1)D] \\ H_{\perp} &= (g_{\perp}/g_{\perp})[H_0 - (2S - 1)D/2] \end{aligned} \quad (4)$$

where $g_{\parallel} = 2.0023$ and \parallel and \perp refer to the directions parallel and perpendicular to the unique axis of the zero-field splitting. It is apparent that for positive D the perpendicular transition is observed at low field and the parallel at high field, while for negative D the reverse is true. Assuming axial zero field splitting, the transitions for the parallel field are spaced by $2D$ and the ones for the perpendicular field by D . Analyses of the obtained spectra led to the following parameters: $g_{\perp} = 2.221$, $g_{\parallel} = 2.055$, and $D = +0.3 \text{ cm}^{-1}$. The corresponding spectra have been calculated considering the zero field splitting as a second order perturbation to the Zeeman term and are shown in Figure 7. The value of D is in agreement with the estimation obtained from the X-band spectra.

In order to calculate the expected transitions for the X-band spectrum it is necessary to diagonalize the Hamiltonian matrix because the strong field approximation does not hold any longer. The calculated EPR spectrum using the parameters obtained from the 245 GHz spectra is shown in Figure 5. The agreement is extremely good.

At first sight the obtained g values are surprising. For a copper(II) ion in a tetragonal pyramidal coordination environment one expects $g_{\parallel} > g_{\perp} > 2.0$. However, the observed g values are the result of the averaging of the individual copper(II) ions of the cluster.¹⁵

We will now assume an idealized D_{6h} symmetry for the cluster and tetragonal pyramidal environments for the copper(II) ions. The local and molecular coordinate systems, hereafter

denoted as xyz and XYZ , have been chosen so that $z \perp Z$ and $x \parallel Z$, where z and Z coincide with the copper(II) pyramidal axis and with the virtual 6-fold axis of the cluster, respectively. Therefore the following relations must hold.

$$\begin{aligned} g_{Z,m} &= g_{x,Cu} \\ g_{X,m} &= \frac{1}{2} (g_{z,Cu} + g_{x,Cu}) \end{aligned} \quad (5)$$

where the subscripts "Cu" and "m" denote local and molecular tensors, respectively.

Using these we calculate $g_{\perp,Cu} = 2.055$ and $g_{\parallel,Cu} = 2.387$, which are comparable to the values of $g_x = 2.08$ and $g_z = 2.40$ for the copper complex $\text{Cu}(\text{apy})_5(\text{ClO}_4)_2$ with a square pyramidal CuO_5 chromophore.¹⁶

The observed zero field splitting must have its origin in the spin-spin determined contribution¹⁷

$$H = \sum_{i=1}^6 \mathbf{S}_i \cdot \mathbf{D}_{i(i+1)} \cdot \mathbf{S}_{i+1} \quad (6)$$

where $i + 1 = 7$ is equivalent to $i = 1$. The observed zero field splitting tensor for the ground $S = 3$ state is given by

$$\mathbf{D} = \sum_{i=1}^6 d_{i(i+1)} \cdot \mathbf{D}_{i(i+1)} \quad (7)$$

Symmetry requires that all the $d_{i(i+1)}$ coefficients are identical to each other. The coefficients can be easily calculated with standard techniques¹⁸ as

$$d_{i(i+1)} = \frac{1}{30} \quad (8)$$

It is now convenient to express the $\mathbf{D}_{i(i+1)}$ tensors in a coordinate frame whose z' axis is directed along one of the lines connecting neighboring copper(II) ions and whose x' axis is parallel to Z . With these assumptions (7) can be written as

$$\begin{aligned} D_{ZZ} &= \frac{1}{5} D_{12,x'x'} \\ D_{XX} &= \frac{1}{10} (D_{12,z'z'} + D_{12,y'y'}) \end{aligned} \quad (9)$$

It is well-known that in copper(II) dimers both exchange and dipolar interactions are important. D^{dip} can be calculated in the approximation of the magnetic dipoles centered on the metal ions.¹⁷ Using the g values obtained for the metal ion, g_{Cu} , leads to the following values of the D^{dip} tensor components

$$\begin{aligned} D_{12,x'x'}^{\text{dip}} &= 0.103 \text{ cm}^{-1} \\ D_{12,y'y'}^{\text{dip}} &= 0.078 \text{ cm}^{-1} \\ D_{12,z'z'}^{\text{dip}} &= -0.181 \text{ cm}^{-1} \end{aligned}$$

Assuming now, that the exchange contribution in the plane $x'y'$ is isotropic, we can calculate $D_{12,z'z'}^{\text{ex}}$, using the dipolar value and eq 9, to be -1.79 cm^{-1} . The exchange determined D component is known to increase rapidly with decreasing

(14) Barra, A. L.; Caneschi, A.; Gatteschi, D.; Sessoli, R. *J. Am. Chem. Soc.* **1995**, *117*, 8855.

(15) Bertini, I.; Gatteschi, D.; Scozzafava, A. *Coord. Chem. Rev.* **1979**, *29*, 67

(16) Srinivasan, R.; Subramanian, C. K. *Indian J. Pure Appl. Phys.* **1970**, *42*, 3693.

(17) Bencini, A.; Gatteschi, D. *EPR of Exchange Coupled Systems*; Springer-Verlag: Berlin, Heidelberg, Germany, 1990.

(18) Abragam, A.; Bleaney, B. *Electron Paramagnetic Resonance of Transition Ions*; Clarendon Press: New York 1970.

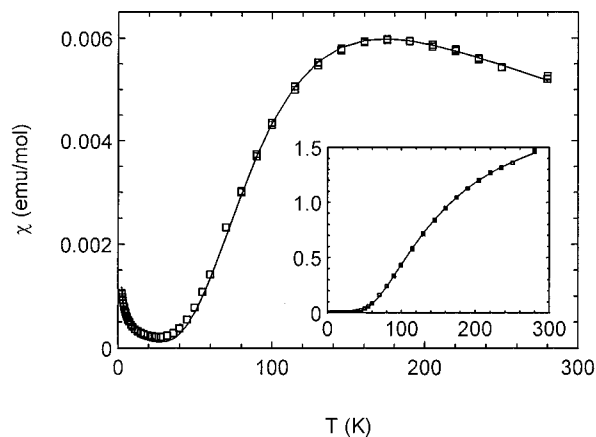


Figure 8. Temperature dependence of χ for compound **2**. In the inset is shown χT vs T . The solid line represents the calculated values with the best fit parameters $J = 193 \text{ cm}^{-1}$, $g = 2.35$, and $\rho = 2.07 \cdot 10^{-3}$ (see also text).

copper–copper distance as observed by Bencini et al.¹⁹ The largest $|D_{zz}^{\text{ex}}|$ value (0.9 cm^{-1}) previously reported corresponds to Cu–Cu = 2.85 \AA . Since the Cu–Cu distance found here (2.79 \AA) is well below the one above, a D_{zz}^{ex} value of at least -1.83 cm^{-1} is a nice confirmation of the outlined exponential dependency of $|D_{zz}^{\text{ex}}|$ on the copper–copper distance. Further, the sign of the exchange-determined component could be unambiguously determined here for the first time, because the sign of D could be determined by HF-EPR.

The magnetic behavior of **2** and **3** is shown in Figures 8 and 9, respectively. The susceptibility of each compound goes through a maximum at around 170 and 175 K, respectively, and decreases rapidly as the temperature is lowered, reaching minimum values at 25 and 30 K. This behavior is consistent with an antiferromagnetic coupling of the Cu atoms in the Cu_2O_6 units. On further cooling, χ increases again due to the presence of a small amount of noncoupled species in the samples. Assuming that the paramagnetic “impurity” follows the Curie law and has the same g factor as the actual compound, it can be easily taken into account, calculating ρ , the molar fraction of noncoupled species. Least squares fittings led to the following best fit parameters: $J = 193(26) \text{ cm}^{-1}$, $g =$

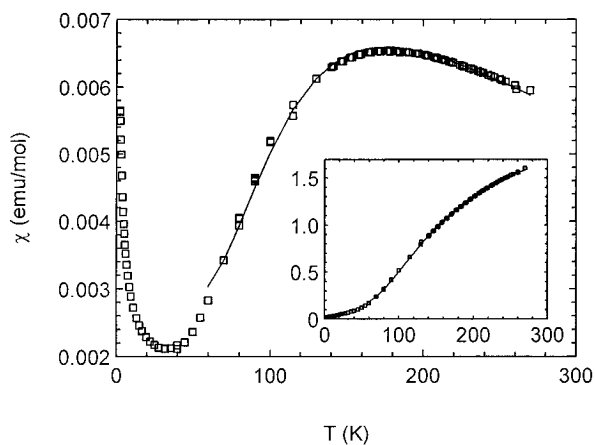


Figure 9. Temperature dependence of χ for compound **3**. In the inset is shown χT vs T . The solid line represents the calculated values with the best fit parameters $J = 210 \text{ cm}^{-1}$, $g = 2.43$, and $\rho = 7.62 \cdot 10^{-2}$ (see also text).

$2.35(16)$, $\rho = 2.07 \times 10^{-3}$ with $R = 6.3 \times 10^{-5}$ for **2**, and $J = 210(24) \text{ cm}^{-1}$, $g = 2.43(15)$, $\rho = 7.62 \times 10^{-2}$ with $R = 9.8 \times 10^{-5}$ for **3**. The high g values reflect some systematic error in the data. However, in contrast to compound **1** the resulting coupling constants are in full agreement with the values predicted by Hatfield and Hodgson.¹³ In our case we should expect values of $J = 255(22) \text{ cm}^{-1}$ for **2** and $J = 219(30) \text{ cm}^{-1}$ for **3**. We can consider the satisfactory agreement as an indication of the similarity of the siloxanolate bridge to the hydroxo bridge.

Acknowledgment. The Human Capital and Mobility Grant ERBCHICT940957 is gratefully acknowledged. Thanks are also due to the “Ministero dell’Università e della Ricerca Scientifica e Tecnologia” (MURST), the National Research Council (CNR) of Italy and the International Science and Technology Center (Grant 15-94) for financial support.

Supporting Information Available: Figure showing calculated EPR spectra of **1** at 245 GHz for 5, 10, 20, 50, and 120 K, assuming $S = 3$, $g_{\perp} = 2.221$, $g_{\parallel} = 2.055$, $D = 0.3 \text{ cm}^{-1}$, $D/E = 0$, and line widths = 300 mT for the transitions perpendicular to the field and 450 mT parallel to the field (1 page). Ordering information is given on any current masthead page.

(19) Bencini, A.; Gatteschi, D.; Zanchini, C.; Haase, W. *Inorg. Chem.* **1985**, *24*, 3485.